World Academy of Science, Engineering and Technology
International Journal of Materials and Metallurgical Engineering
Vol:13, No:12, 2019

Synthesis, Structure and Properties of NZP/NASICON Structured Materials

E. A. Asabina, V. I. Pet'kov, P. A. Mayorov, A. V. Markin, N. N. Smirnova, A. M. Kovalskii, A. A. Usenko

***Abstract*—**The purpose of this work was to synthesize and investigate phase formation, structure and thermophysical properties of the phosphates $M_{0.5+x}M'_xZr_{2-x}(PO_4)_3$ (M – Cd, Sr, Pb; M' – Mg, Co, Mn). The compounds were synthesized by sol-gel method. The results showed formation of limited solid solutions of NZP/NASICON type. The crystal structures of triple phosphates of the compositions $MMg_{0.5}Zr_{1.5}(PO_4)_3$ were refined by the Rietveld method using XRD data. Heat capacity (8–660 K) of the phosphates $Pb_{0.5+x}Mg_xZr_{2-x}(PO_4)_3$ (x = 0, 0.5) was measured, and reversible polymorphic transitions were found at temperatures, close to the room temperature. The results of Rietveld structure refinement showed the polymorphism caused by disordering of lead cations in the cavities of NZP/NASICON structure. Thermal expansion (298−1073 K) of the phosphates $MMg_{0.5}Zr_{1.5}(PO_4)_3$ was studied by XRD method, and the compounds were found to belong to middle and low-expanding materials. Thermal diffusivity (298–573 K) of the ceramic samples of phosphates slightly decreased with temperature increasing. As was demonstrated, the studied phosphates are characterized by the better thermophysical characteristics than widespread fire-resistant materials, such as zirconia and etc.

***Keywords*—**NASICON, NZP, phosphate, structure, synthesis, thermophysical properties.

I. Introduction

THE materials of the NASICON (sodium superionic conductor) or the NZP (sodium zirconium phosphate) family are very attractive because of their compositional diversity leading to many possible applications. These ceramics have been shown to possess such industrially useful properties, as fast ion conduction and low thermal expansion [1]-[8]. Previous studies carried out on certain members of this structural family have also shown prospects for use as solid catalysts of alcohols' conversion [9].

The derivative materials that have been extensively studied are $M_{0.5}Zr_2(PO_4)_3$ (M – Ca, Cd, Sr, Pb, Ba) [8], [10]-[14], which are isostructural with NZP/NASICON. The compounds have high-temperature stability and excellent thermal shock resistance, which renders the materials to be a potential candidate for host of applications such as radioactive waste isolation, thermal shock barrier coating, automobile engine component, and catalyst supports. They are characterized by very low average bulk thermal expansion and exhibit an anisotropy in the thermal expansion, which lowers the bulk thermal expansion of the polycrystalline material through micromechanical stress induced-microcracking during cooling from the processing temperature [10].

The phases $M_{0.5}Zr_2(PO_4)_3$ (M – Ni, Mg, Co, Cu, Mn) [14] were found to be a part of scandium tungstate (SW) family structurally related to NZP/NASICON. The both crystal structures are composed of PO_4 tetrahedra that corner share O^{2-}-anions with neighboring ZrO_6 octahedra to produce a rigid three-dimensional framework. Interstitial M^{2+} cations within the framework can occupy distinct, distorted 6- and 8-coordinated voids (medium and large cations) of the NZP/NASICON structure or 4-fold ones (small ions) of the SW. However, results of the solid solutions $M_{0.5+x}M'_xZr_{2-x}(PO_4)_3$ (M – Co, Mn, Ca, Ba; M' – Ni, Mg, Cu, Co, Mn) study [15] have shown that the NZP/NASICON compounds were characterized by higher thermal stability compared with the SW ones. Besides, NZP/NASICON compounds usually have lower thermal expansion coefficients.

The purpose of this work was to synthesize and investigate experimentally phase formation, structure and thermophysical properties of the phosphates $M_{0.5+x}M'_xZr_{2-x}(PO_4)_3$ (M – Cd, Sr, Pb; M' – Mg, Co, Mn).

II. Experimental Procedure

A. Samples Preparation

All compositions were synthesized via conventional sol-gel method [15]. The following starting reactants had been used: CdO, $Sr(NO_3)_2$, $Pb(NO_3)_2$, MgO, $CoCl_2{\cdot}6H_2O$, $Mn(CH_3COO)_2{\cdot}4H_2O$, $ZrOCl_2{\cdot}8H_2O$, $NH_4H_2PO_4$. All the reactants had been provided by Reachem and had a purity not less than 99.5% (except of $ZrOCl_2{\cdot}8H_2O$, 99.0%). Before synthesis, the salts had been dissolved in the distilled water, the oxides – in the aqueous solutions of hydrochloric acid. Zirconium concentration in the solution was additionally determined gravimetrically with cupferron [16].

During synthesis of each sample, a stoichiometric amount of $NH_4H_2PO_4$ solution was dropped into homogenized mixture of other salts' solutions taken in necessary amounts. Then the obtained compound was heated at 363 K for 24 h to vaporize water. After grinding, the powder was again annealed for 50 h at the steps between 873 K and 1323 K depending on the composition [15].

E. A. Asabina is with the Chemical Department, Lobachevsky University, Nizhny Novgorod 603950, Russia (corresponding author, phone: +7-831-4623234; e-mail: elena.asabina@inbox.ru).

V. I. Pet'kov, P. A. Mayorov, and A. V. Markin are with the Chemical Department, Lobachevsky University, Nizhny Novgorod 603950, Russia (e-mail: petkov@inbox.ru, pavel.mayorov.94@mail.ru, markin79@mail.ru).

N. N. Smirnova is with the Chemical Department, Lobachevsky University, Nizhny Novgorod 603950, Russia.

A. M. Kovalsky is with the National University of Science and Technology MISIS, Moscow 119049, Russia (e-mail: andreykovalskii@gmail.com).

A. A. Usenko is with the National University of Science and Technology MISIS, Moscow 119049, Russia.

This work was supported by the Russian Foundation for Basic Research, Projects no. 18-29-12063, 19-33-90075.

B. Measurement and Characterization

The synthesized samples were characterized by X-ray powder diffraction (XRD) on a Shimadzu XRD-6000 diffractometer using CuK_α, X-ray beam (λ = 1.54178 Å). The diffraction patterns were obtained in 2θ range 10–60 deg. in continuous scan mode with detector velocity 0.5 deg./min and step recording every 0.02 deg. The indexing was performed by comparing the interplanar crystal spacing d and intensities of reflections I of the investigated samples with literature data [15], [17], [18]. The thermal expansion of the polycrystalline ceramics was measured using XRD method in the same conditions at temperatures from 298 K to 1073 K. The XRD patterns for Rietveld refinement were collected in fixed time mode. The experimental details for each sample are given in the Results and Discussion section. The crystal structures of the samples were refined using Rietan-97 program [19].

IR spectra of the compounds prepared as pellets (with KBr) were recorded on a Shimadzu FTIR 8400S spectrometer in the range 1400-400 cm^{-1} (resolution 4 cm^{-1}).

The elemental and phase compositions of the prepared materials were examined using a JSM-7600F Schottky field emission scanning electron microscope (JEOL) equipped with microanalysis system with energy-dispersive X-ray (EDX) detector OXFORD X-Max 80 Premium (Oxford Instruments).

The acceleration voltage was (15 and 20) kV. The accuracy of elements content' determination was 0.5–2.0 at.%.

A precision automatic adiabatic calorimeter BCT-3 (Termis) [20] with discrete heating was used to measure heat capacity of the $Pb_{0.5}Zr_2(PO_4)_3$ in the temperature range 8–300 K. Liquid helium and nitrogen were used as cooling agents. The reliability of the measurements was verified by determination of heat capacity of high-pure copper, K-2 benzoic acid and synthetic corundum, prepared at the Institute of Metrology of the State Standard Committee of the Russian Federation. It was found that error of heat capacity measurement was ±2% up to 15 K, then it decreased to ±0.5% as the temperature was rising to 40 K, and was equal to ±0.2 K over the temperature range 40–350 K. The accuracy of phase transitions' temperatures was 0.01 K, and the standard uncertainty of transitions' enthalpies was ±0.2%. The ampule of the adiabatic calorimeter contained 1.47266 g of the studied sample.

A differential scanning calorimeter DSC 204 F1 Phoenix with μ-sensor (Netzsch) [21], [22] was applied to measure the heat capacity of the phosphates in the temperature interval 195–660 K. The calorimeter was calibrated and tested using melting temperatures of n-heptane, mercury, tin, lead, bismuth, and zinc. The equipment and a measurement technique allow to measure temperatures of phase transitions with error ±0.5 K, enthalpy of transitions ±1%. Heat capacity of the samples was measured at the heating rate 5 $K \cdot min^{-1}$ in argon atmosphere, the error of definition did not exceed ±2%.

The thermal diffusivity of the ceramics was measured by laser flash method in the temperature range 298–473 K using a LFA447 NanoFlash device (Netzsch). The relative density of ceramic samples was ~ 80%. In our measurements, the front side of the sample (12.7 mm in diameter and ~2 mm in thickness) was heated by a short laser pulse. After the absorption of the pulse energy in the sample, the temperature profile across it flattened out. In this process, the relative temperature change on the rear surface of the sample was measured using an IR detector. A mathematical analysis of temperature time variation under adiabatic conditions allowed us to determine thermal diffusivity a: $a = 0.1388 \cdot l^2/\tau_{0.5}$, where l (mm) is the thickness of the sample and $\tau_{0.5}$ (s) is the time needed for 50% of the maximum temperature to be reached. The uncertainty of determination did not exceed ±5%. Thermal conductivity λ was calculated as $\lambda = a \cdot \rho \cdot C_{p,}^0$, where ρ (g/cm^3) is the density of the sample and C_p^0 (J/(g·K)) is its heat capacity.

III. Results and Discussion

A. Phase Formation and Structure

According to the results of XRD, IR spectroscopy and electron EDX microanalysis, NZP/NASICON solid solutions were obtained in all the studied series of phosphates $M_{0.5+x}M'_xZr_{2-x}(PO_4)_3$ (M – Cd, Sr, Pb; M' – Mg, Co, Mn) [15].

Fig. 1 (a) shows the XRD results for the synthesized $Cd_{0.5+x}Mg_xZr_{2-x}(PO_4)_3$ phases. The limited solid solution was obtained in the range $0 \le x \le 0.6$ at the temperature of synthesis 973 K. The XRD patterns of these phosphates were analogous to the literature data on the NZP/NASICON type compound $Cd_{0.5}Zr_2(PO_4)_3$ [17] and were indexed in space group $R\bar{3}$. The appearance of additional reflections in the XRD patterns of the samples with $0.7 \le x \le 2.0$ indicates the presence of the phases of cadmium and magnesium phosphates.

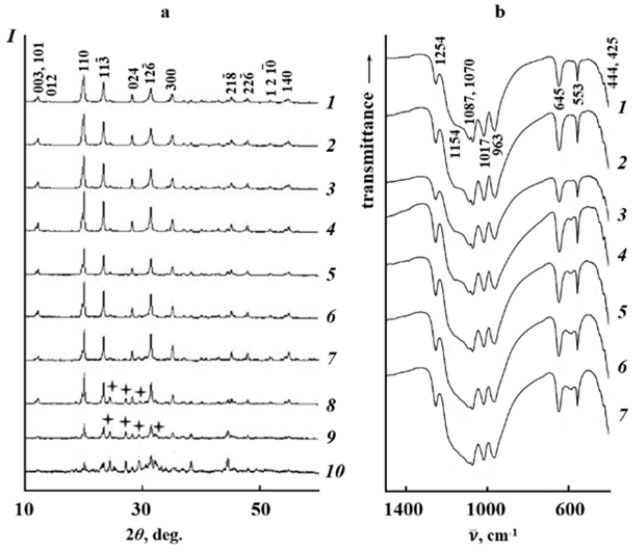

Fig. 1 XRD patterns (a) and IR spectra (b) of the phosphates $Cd_{0.5+x}Mg_xZr_{2-x}(PO_4)_3$: x = 0 (*1*), 0.1 (*2*), 0.2 (*3*), 0.3 (*4*), 0.4 (*5*), 0.5 (*6*), 0.6 (*7*), 0.7 (*8*), 1.0 (*9*), 2.0 (*10*). Reflections corresponding to cadmium and magnesium phosphates are shown with ✦

The IR spectra of the obtained compounds (Fig. 1 (b)) were similar and contained absorption bands characteristic (in shape

and positions) for the NZP/NASICON phosphates. As it is often observed, the realized number of absorption bands is less than the theoretical one: 6 bands of stretching (1260–1000 cm^{-1}) and bending asymmetric vibrations (650–540 cm^{-1}), 2 bands of symmetric stretching (1000–900 cm^{-1}) and 4 symmetrical bending vibrations (below 500 cm^{-1}) of PO_4^{3-} tetrahedra.

Fig. 2 shows SEM image of the synthesized NZP/NASICON compound surface. The image reveals a homogeneous microporous structure made of agglomerated particles around 1–20 μm large. Chemical formulae of the prepared material predicted on the base of EDX investigation (Table I) confirm that its composition corresponds to the theoretical one for the formula $CdMg_{0.5}Zr_{1.5}P_3O_{12}$.

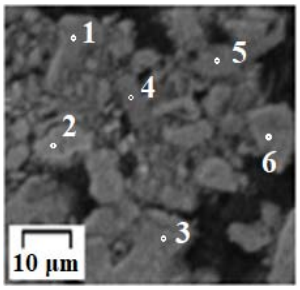

Fig. 2 SEM image of the phase with the theoretical composition $CdMg_{0.5}Zr_{1.5}P_3O_{12}$

TABLE I
RESULTS OF ELEMENTAL ANALYSIS FOR THE PHASE WITH THE THEORETICAL COMPOSITION $CdMg_{0.5}Zr_{1.5}P_3O_{12}$

Point Number	O	Cd[a]	Mg	Zr	P
1	12	0.99	0.48	1.43	3.07
2	12	0.97	0.47	1.40	3.10
3	12	0.95	0.45	1.45	3.08
4	12	0.96	0.46	1.48	3.04
5	12	0.99	0.49	1.47	3.03
6	12	1.02	0.49	1.49	3.01
Average	12	0.98(3)	0.47(2)	1.45(4)	3.05(4)

[a]The formula composition was normalized to 12 oxygen atoms.

The other cadmium-containing systems (M' – Co, Mn) showed smaller limits of the NZP/NASICON solid solutions ($0 \le x \le 0.3$) compared with the Cd-Mg-Zr raw. Single-phase products were formed at 973 K. The reason of the difference in solid solution's limits is probably the distinction between Mg^{2+}, Co^{2+} and Mn^{2+} ionic radii.

As evident from Table II, the same tendency is observed in all the studied systems. In fact, increase in M'^{2+} radius in the phosphates $M_{0.5+x}M'_xZr_{2-x}(PO_4)_3$ (M – Cd, Sr, Pb; M' – Mg, Co, Mn) lead to reduction on NZP/NASICON structure limits.

With the aim of making distribution of M, M' metals in the crystallographic sites (framework and cavities) clear, we refined the crystal structures of triple phosphates of the compositions $MMg_{0.5}Zr_{1.5}(PO_4)_3$ ($x = 0.5$) where M – Cd and Sr by the Rietveld method using XRD data. The experimental and refinement conditions are presented in Table III in details. As it is seen from Fig. 3, good agreement between calculated and experimental XRD patterns was reached.

TABLE II
NZP/NASICON SOLID SOLUTIONS' LIMITS IN THE SYSTEMS $M_{0.5+x}M'_xZr_{2-x}(PO_4)_3$

System	x limits
$Cd_{0.5+x}Mg_xZr_{2-x}(PO_4)_3$	$0 \le x \le 0.6$
$Cd_{0.5+x}Co_xZr_{2-x}(PO_4)_3$	$0 \le x \le 0.3$
$Cd_{0.5+x}Mn_xZr_{2-x}(PO_4)_3$	$0 \le x \le 0.3$
$Sr_{0.5+x}Mg_xZr_{2-x}(PO_4)_3$	$0 \le x \le 0.5$
$Sr_{0.5+x}Co_xZr2\text{-}x(PO_4)_3$	$0 \le x \le 0.5$
$Sr_{0.5+x}Mn_xZr_{2-x}(PO_4)_3$	$0 \le x \le 0.3$
$Pb_{0.5+x}Mg_xZr_{2-x}(PO_4)_3$	$0 \le x \le 0.7$
$Pb_{0.5+x}Co_xZr_{2-x}(PO_4)_3$	$0 \le x \le 0.6$
$Pb_{0.5+x}Mn_xZr_{2-x}(PO_4)_3$	$0 \le x \le 0.6$

TABLE III
THE EXPERIMENTAL CONDITIONS AND REFINEMENT DETAILS FOR THE RIETVELD ANALYSIS OF THE PHOSPHATES $MMg_{0.5}Zr_{1.5}(PO_4)_3$ STRUCTURES

M	Cd	Sr
Space Group	$R\bar{3}$	
Z	6	
2θ range, deg.	10–110	
Lattice Parameters:		
a, Å	8.8327(4)	8.7053(4)
c, Å	22.2416(8)	23.3048(7)
V, Å^3	1502.73(11)	1529.5(10)
Reflections number	424	437
Variables:		
Structural	28	28
Other	20	19
R_{wp}, %	7.41	7.65
R_p, %	5.05	5.59

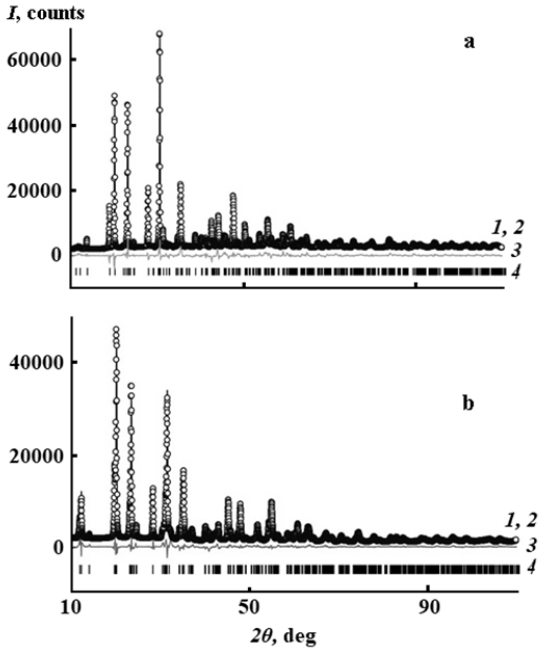

Fig. 3 Observed (*1*), calculated (*2*), difference (*3*) Rietveld refinement profiles and Bragg reflections (*4*) for XRD patterns of the studied phosphates $MMg_{0.5}Zr_{1.5}(PO_4)_3$ with M – Cd (a) and Sr (b)

The initial coordinates for refinement were those of $Cd_{0.5}Zr_2(PO_4)_3$ (NZP/NASICON, space group $R\bar{3}$, [17]). Crystal structures of both phosphates $MMg_{0.5}Zr_{1.5}(PO_4)_3$ (M –

Cd, Sr) may be represented as the frameworks of octahedra and PO_4-tetrahedra that form ribbons along the *c* axis, and there are ions situated in the cavities within the ribbons (Fig. 4). There are two types of framework-forming cationic sites with 6-fold coordination in their structure. In the Sr-compound (Table IV), these positions are occupied by Zr^{4+} and Mg^{2+}/Zr^{4+} ions, and Sr^{2+} cations are distributed in the framework cavities. Unusual cationic distribution was discovered for the Cd-compound's structure: its framework is built up from polyhedra formed by Zr^{4+} and Cd^{2+}/Zr^{4+} ions (together with PO_4), while its cavities are filled with Cd^{2+} and Mg^{2+} cations. Including of Cd^{2+} instead of Mg^{2+} into the framework sites may probably be explained by the closeness of electronic structure of Cd^{2+} and Zr^{4+} (d-elements), that have a stronger influence on the structure formation compared with size factor. As for the Sr-compound, large ionic radius of strontium ions ($r(Sr^{2+}) = 1.18$ Å, $r(Cd^{2+}) = 0.95$ Å) is favorable factor for occupation of cavities but adverse for framework sites.

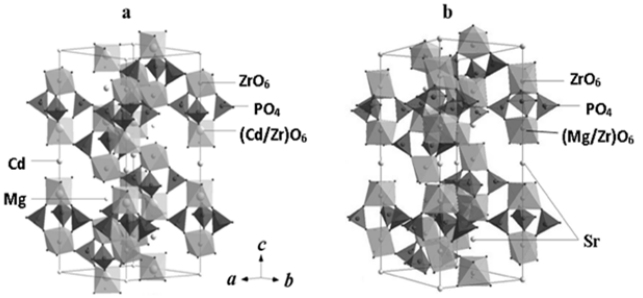

Fig. 4 Crystal structures of the phosphates $MMg_{0.5}Zr_{1.5}(PO_4)_3$ where M – Cd (a) and Sr (b)

TABLE IV
FRACTIONAL COORDINATES AND ISOTROPIC ATOMIC DISPLACEMENT PARAMETERS FOR THE PHOSPHATES $Mmg_{0.5}zr_{2.5}(Po_4)_3$ STRUCTURES

Atom/ Site	*x*		*y*		*z*	
	M – Cd	M - Sr	M – Cd	M – Sr	M – Cd	M – Sr
M(I)[a]/3*a*	0	0	0	0	0	0
M(II)/3*b*	0	0	0	0	0.5	0.5
L(1)/6c	0	0	0	0	0.1346(2)	0.1488(4)
L(2)/6*c*	0	0	0	0	0.6488(2)	0.6497(3)
P/18*e*	0.2855(5)	0.2846(4)	-0.0028(3)	-0.0021(4)	0.2482(4)	0.2492(5)
O(1)/18*f*	0.1886(6)	0.1739(5)	-0.0306(4)	-0.0162(3)	0.1912(5)	0.1982(4)
O(2)/18*f*	-0.0048(6)	0.0568(5)	-0.1837(4)	-0.1879(5)	0.6914(6)	0.6930(3)
O(3)/18*f*	0.2023(4)	0.1900(4)	0.1862(4)	0.1601(5)	0.0901(5)	0.0806(4)
O(4)/18*f*	-0.1650(5)	-0.1661(4)	-0.2038(4)	-0.1989(5)	0.5811(5)	0.5850(4)

[a]In the $CdMg_{0.5}Zr_{1.5}(PO_4)_3$ structure M(I) site is occupied by Mg^{2+}, M(II) site – by Cd^{2+}, L(I) – Zr^{4+}, L(II) – Cd^{2+}/Zr^{4+}. In the $SrMg_{0.5}Zr_{1.5}(PO_4)_3$ structure M(I) and M(II) sites are occupied by Sr^{2+}, L(I) – Mg^{2+}/Zr^{4+}, L(II) – Zr^{4+}.

The bond lengths in the polyhedra forming the studied structures (Table V) were in agreement with the corresponding literature data for other NZP/NASICON phosphates [15], [17], [18]. Note, that the larger scale dispersion of interatomic distances was observed within the (Cd^{2+}/Zr^{4+})-octahedra compared with the (Mg^{2+}/Zr^{4+})-ones, due to difference of Cd^{2+} and Zr^{4+} ionic radii.

Taking into account the obtained structural data, we can discuss limits of NZP/NASICON structure solid solutions listed in Table II. Obviously, closeness in Mg^{2+} and Zr^{4+} radii is propitious for their isomorphic mixing in the systems containing large M^{2+} (Sr^{2+} and Pb^{2+}) ions. So solid solutions' limits decrease with growth of difference in radii of framework-forming ions. The exception is Cd-systems, where Cd^{2+} ions take part in the framework formation according to the undertaken structure refinement.

TABLE V
THE BOND LENGTHS IN THE STRUCTURE-FORMING POLYHEDRA OF THE PHOSPHATES $MMg_{0.5}Zr_{2.5}(PO_4)_3$

$CdMg_{0.5}Zr_{1.5}(PO_4)_3$		$SrMg_{0.5}Zr_{1.5}(PO_4)_3$	
Bond	*d*, Å	Bond	*d*, Å
Cd/Zr–O(2) (x3)	1.861(9)	Mg/Zr–O(1) (x3)	1.962(8)
Cd/Zr–O(4) (x3)	2.238(9)	Mg/Zr–O(3) (x3)	2.213(9)
Zr–O(3) (x3)	1.985(6)	Zr–O(2) (x3)	2.179(5)
Zr–O(1) (x3)	2.209(7)	Zr–O(4) (x3)	2.204(8)
P(1)–O(3)	1.473(4)	P(1)–O(1)	1.496(12)
P(1)–O(1)	1.480(13)	P(1)–O(4)	1.513(6)
P(1)–O(4)	1.504(6)	P(1)–O(2)	1.542(12)
P(1)–O(2)	1.636(14)	P(1)–O(3)	1.607(4)

Despite that difference, dependences of the lattice parameters against composition for all the studied systems $M_{0.5+x}M'_xZr_{2-x}(PO_4)_3$ were similar and typical for NZP/NASICON series (Fig. 5). As large (Cd^{2+}) ions are incorporated in the structure, monotonous growth of *c* parameter is observed. As a rule, this effect is accompanied by correlated tilt of the framework-forming polyhedra, leading to reduction in *a* parameter [8].

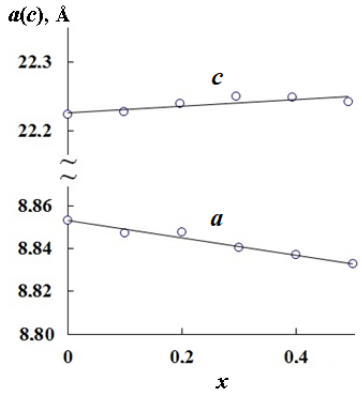

Fig. 5 Lattice parameters against composition for the phosphates $CdMg_{0.5}Zr_{1.5}(PO_4)_3$

B. Thermal Expansion

Many NZP/NASICON phosphates are characterized by low average expansion coefficients. To control thermal expansion, it is important to reveal the influence of various factors on NZP/NASICON structure deformations during heating. As the compounds $M_{0.5}Zr_2(PO_4)_3$ (x = 0) are well-known in literature and their thermal expansion was widely studied (Table VI, [8]), we present here the results of the thermal expansion study for the phosphates $MMg_{0.5}Zr_{1.5}(PO_4)_3$ (M – Cd, Sr; x = 0.5).

The compounds were investigated by high-temperature XRD within the temperature range 298–1073 K. The temperature dependences of their lattice parameters may be described by the linear functions given in Table VII.

According to the calculations, $CdMg_{0.5}Zr_{1.5}(PO_4)_3$ is characterized by negative α_a (due to tilt of the framework polyhedra) and significantly high positive α_c expansion coefficients. As for $PbMg_{0.5}Zr_{1.5}(PO_4)_3$, the both observed thermal expansion coefficients are positive, anisotropy is low and the α_{av} allows us to classify it as low-expanding material. The reason is apparently that the presence of large Pb^{2+} cations in the structural cavities lead to significant deformation of the framework at room temperature, so further deformation of structure during heating is suppressed. A general tendency for NZP/NASICON materials is observed: the incorporation of a larger cation into the structural cavities reduces both thermal expansion and thermal expansion anisotropy. Comparison of Tables VI and VII illustrates for the example of cadmium system that the increase in cavities occupation weak influence on the phosphate thermal expansion.

TABLE VI
THERMAL EXPANSION OF THE PHOSPHATES $M_{0.5}Zr_2(PO_4)_3$ ACCORDING TO THE LITERATURE DATA [8]

M	r, Å	$\alpha \cdot 10^6$, K^{-1}			
		α_a	α_c	$\lvert\alpha_a - \alpha_c\rvert$	α_{av}
Cd	0.95	–3.50	10.20	13.7	1.07
Ca	1.00	–2.57	7.74	10.3	0.87
Sr	1.18	2.24	2.28	0.0	2.25

TABLE VII
THERMAL EXPANSION OF THE PHOSPHATES $MdMg_{0.5}Zr_{1.5}(PO_4)_3$ WITHIN THE RANGE 298–1073 K

M	r, Å	Functions a, c (Å) = $f(T, K)$	$\alpha \cdot 10^6$, K^{-1}			
			α_a	α_c	$\lvert\alpha_a - \alpha_c\rvert$	α_{av}
Cd	0.95	$a = 3 \cdot 10^{-5} T + 8.8238$ $c = 3 \cdot 10^{-4} T + 22.152$	–3.2	13.9	17.1	2.5
Pb	1.19	$a = 2 \cdot 10^{-5} T + 8.6937$ $c = 6 \cdot 10^{-5} T + 23.441$	1.9	2.6	0.7	2.2

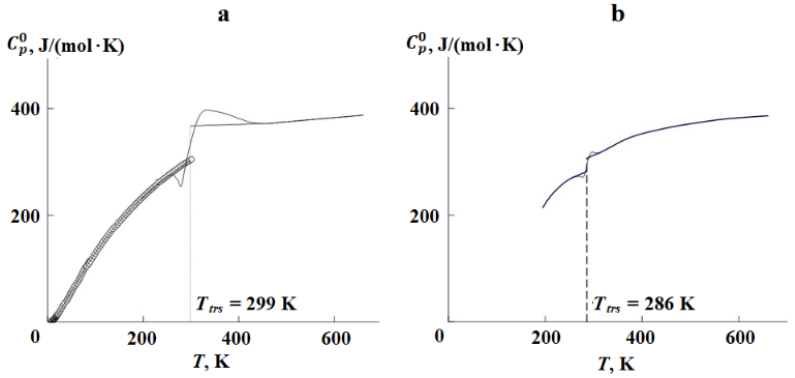

Fig. 6 Crystal structures of the phosphates $Pb_{0.5+x}Mg_xZr_{2-x}(PO_4)_3$ where $x = 0$ (a) and 0.5 (b)

C. Heat Capacity and Phase Transitions

Heat capacities and phase transitions of the crystalline phosphates $Pb_{0.5+x}Mg_xZr_{2-x}(PO_4)_3$ (x = 0, 0.5) were studied (Fig. 6). The measurements of $Pb_{0.5}Zr_2(PO_4)_3$ heat capacity were performed by adiabatic vacuum (8–300 K, 110 experimental C_p^0 values) and differential scanning calorimetry (constant heating rate, 195–660 K). The sample $PbMg_{0.5}Zr_{1.5}(PO_4)_3$ was studied by differential scanning calorimetry (195–660 K). The experimental C_p^0 values were smoothed using power and semilogarithmic polynomials. According to the obtained data, the studied phosphates undergo reversible phase transitions (256–426 K for $Pb_{0.5}Zr_2(PO_4)_3$ and 255–315 K for $PbMg_{0.5}Zr_{1.5}(PO_4)_3$), that may be attributed to *G*-type transitions. Note, that during measurements of heat capacity of the $Pb_{0.5}Zr_2(PO_4)_3$ sample in the adiabatic calorimeter, the transition did not appear up to 300 K, that is probably caused by its nonequilibrium character (the transition does not appear under the conditions close to equilibrium).

To study the nature of the considered phase transformations, structural study of $Pb_{0.5}Zr_2(PO_4)_3$ was carried out at temperatures T = 173 and 473 K by the Rietveld method using powder XRD data (Fig. 7, Table VIII). The atomic coordinates in the structure of the phosphate $Cu_{0.25}Mn_{0.25}Zr_2(PO_4)_3$ [23] were used as the starting model.

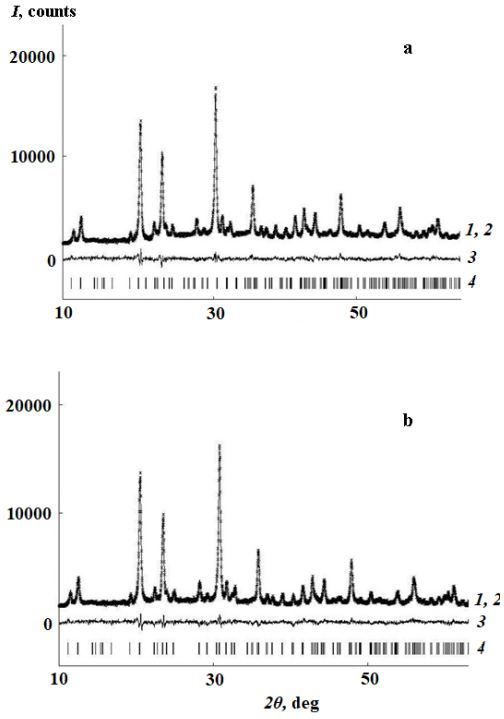

Fig. 7 Observed (*1*), calculated (*2*), difference (*3*) Rietveld refinement profiles and Bragg reflections (*4*) for XRD patterns of the studied phosphate $Pb_{0.5}Zr_2(PO_4)_3$ at T = 173 (a) and 473 K (b)

TABLE VIII
THE EXPERIMENTAL CONDITIONS AND REFINEMENT DETAILS FOR THE RIETVELD ANALYSIS OF THE PHOSPHATE $Pb_{0.5}Zr_2(PO_4)_3$ STRUCTURES

T, K	173	473
Space Group	$R\bar{3}$	
Z	6	
2θ range, deg.	10–80	
Lattice Parameters:		
a, Å	8.7009(4)	8.6996(16)
c, Å	23.4822(11)	23.479(3)
V, Å^3	1539.57(13)	1538.9(4)
Reflections number	295	301
Variables:		
Structural	28	28
Other	23	23
R_{wp}, %	3.47	3.48
R_p, %	2.75	2.75

From the results (Fig. 8, Tables IX, X), both polymorphic forms of $Pb_{0.5}Zr_2(PO_4)_3$ belong to NZP/ NASICON type structure and crystallize in the same space group $R\bar{3}$. In the structures of most NZP/NASICON compounds of the composition $M_{0.5}Zr_2(PO_4)_3$ [14], M^{2+} cations occupy cavities sites (3*a* or 3*b*, within the polyhedra columns) characterized by an octahedral coordination with 6 M–O bonds of the same length. The $Pb_{0.5}Zr_2(PO_4)_3$ structure differs from them in Pb^{2+} location. The Pb^{2+} ions have a stereoactive $6s^2$ electron pair, which usually leads to distortion of PbO_6 polyhedra [24]. As a result, Pb^{2+} ions are displaced from the centers of octahedrally coordinated cavities (disordered) and the symmetry of their positions decreases to 18*f*. The degree of the polyhedra distortion in known Pb-containing compounds depends on the temperature and structural features of the substances. The results of the $Pb_{0.5}Zr_2(PO_4)_3$ structure Rietveld refinement at 173 K and 473 K evident that increase of distortion of the PbO_6 octahedra is observed with growth of temperature. Thus, polymorphic transitions on the heat capacity curves of the studied phosphates are caused by disordering of Pb^{2+} cations in the cavities of NZP/NASICON structure. Lower interval of transition temperatures for $PbMg_{0.5}Zr_{1.5}(PO_4)_3$ compared with $Pb_{0.5}Zr_2(PO_4)_3$ can be explained by the fact that, in its structure, Pb^{2+} cations completely occupy the cavities within the columns of framework-forming polyhedra and, therefore, there are less possibilities of these ions displacement and corresponding structural deformations.

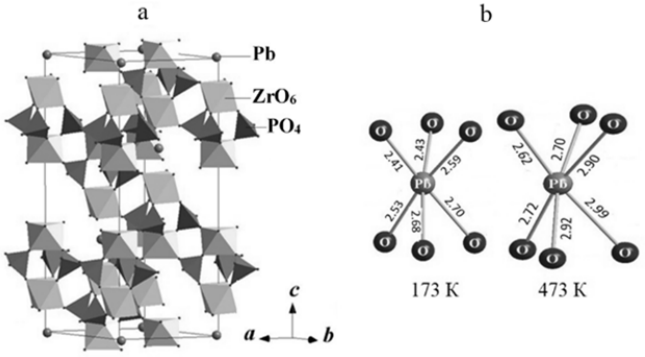

Fig. 8 Crystal structures of the phosphate $Pb_{0.5}Zr_2(PO_4)_3$ at 173 K (a) and distortion of PbO_6 polyhedra at 173 and 473 K (b)

TABLE IX
FRACTIONAL ATOMIC COORDINATES FOR THE $Pb_{0.5}Zr_2(PO_4)_3$ STRUCTURE

Atom/ Site	*x*		*y*		*z*	
	173 K	473 K	173 K	473 K	173 K	473 K
Pb[a]/18*f*	0.02(6)	-0.033 (26)	0.00(12)	-0.034(22)	0.0044(11)	0.0035(13)
Zr(1)/6c	0	0	0	0	0.15061(18)	0.15073(20)
Zr(2)/6*c*	0	0	0	0	0.64726(17)	0.64701(19)
P/18*e*	0.2939(13)	0.2996(13)	0.0201(16)	1.0237(15)	0.2524(6)	0.2455(6)
O(1)/18*f*	0.1701(21)	0.1655(23)	0.9654(22)	0.9585(26)	0.1901(11)	0.1927(10)
O(2)/18*f*	0.073(3)	0.1513(25)	0.859(3)	0.9306(23)	0.7036(7)	0.7024(8)
O(3)/18*f*	0.193(3)	0.2022(25)	0.178(2)	0.1516(22)	0.0840(9)	0.0980(8)
O(4)/18*f*	0.8293(28)	0.7999(26)	0.7724(23)	0.7733(27)	0.6114(8)	0.5936(8)

[a]Occupancy 0.167.

To calculate thermodynamic functions of the phosphate $Pb_{0.5}Zr_2(PO_4)_3$, the temperature dependence of its heat capacity was extrapolated to 0 K using the Debye function: C_p^0 = nD(θD/T), where D is the symbol of the Debye function, n = 3 and θD = 88.4 K – selected parameters. With the indicated parameters, this equation describes the experimental values in the region of 8–12 K with an uncertainty of 2.4%. It was believed that the equation reproduces the values of at T < 8 K with the same accuracy.

The values of enthalpies $[H^0(T) - H^0(0)]$ and entropies $S^0(T)$ for the compound Pb0.5Zr2(PO4)3 (Table XI) were calculated by numerical integration of the dependences C_p^0 = f(T) and C_p^0 = f(lnT), the Gibbs functions $[G^0(T) - H^0(0)]$ were obtained from the values of enthalpies and entropies at the corresponding temperatures. The heat capacity values of $PbMg_{0.5}Zr_{1.5}(PO_4)_3$ smoothed using polynomials are given in Table XII.

Note that heat capacity of the studied phosphates at high temperatures approaches the values estimated by the Dulong and Petit rule: $C_p^0 = 3RN$, where R is the universal gas constant, N is the number of atoms in the formula unit. The calculated and experimental (at 660 K) heat capacities were 436.5 and 387.8 J/(mol·K) for $Pb_{0.5}Zr_2(PO_4)_3$, 449.0 and 416 J/(mol·K) for $PbMg_{0.5}Zr_{1.5}(PO_4)_3$.

TABLE X
THE BOND LENGTHS IN THE STRUCTURE-FORMING POLYHEDRA OF THE PHOSPHATE $Pb_{0.5}Zr_2(PO_4)_3$

Bond	*d*, Å	
	173 K	473 K
Pb–O(3)	2.41(3)	2.62(2)
Pb–O(3')	2.43(6)	2.70(5)
Pb–O(3'')	2.53(4)	2.72(8)
Pb–O(3''')	2.59(5)	2.90(7)
Pb–O(3'''')	2.68(6)	2.92(5)
Pb–O(3''''')	2.70(3)	2.99(6)
Zr(1)–O(1) (×3)	1.894(21)	1.922(23)
Zr(1)–O(3) (×3)	2.250(19)	2.012(17)
Zr(1)–O(4) (×3)	1.974(23)	2.141(19)
Zr(1)–O(2) (×3)	2.107(27)	2.252(19)
P–O(3)	1.413(21)	1.426(17)
P–O(2)	1.443(29)	1.436(12)
P–O(4)	1.535 (26)	1.599(25)
P–O(1)	1.636(27)	1.699(27)

TABLE XI
STANDARD THERMODYNAMIC FUNCTIONS OF THE CRYSTALLINE $Pb_{0.5}Zr_2(PO_4)_3$

T, K	C_p^0, J/(mol·K)	$[H^0(T)-H^0(0)]$, kJ/mol	$S^0(T)$, J/(mol·K)	$-[G^0(T)-H^0(0)]$, kJ/mol
Crystal I				
0	0	0	0	0
100	129.5	5.822	96.29	3.807
298.15	303.4	50.99	328.2	46.87
299	303.9	51.24	329.1	47.15
Crystal II				
299	367.7	51.24	329.1	47.15
300	368	51.6	330	47.5
400	370	88.5	436	86.1
500	375	126	520	134
600	383	164	589	190
660	388	187	625	226

TABLE XII
STANDARD HEAT CAPACITY OF THE CRYSTALLINE $PbMg_{0.5}Zr_{1.5}(PO_4)_3$

T, K	C_p^0, J/(mol·K)
Crystal I	
195	214
200	222
286	282
Crystal II	
286	307
298.15	312
300	312
400	353
500	371
600	383
660	386

C. Thermal Diffusivity (Conductivity)

Thermal diffusivity of the ceramics $M_{0.5}$+xMgxZr_2–x$(PO_4)_3$ (M – Cd, Pb; x = 0, 0.5) was measured in the temperature range 298-473 K (Fig. 9). As a characteristic feature of ceramics, a slight monotonous decrease in the thermal diffusivity was observed with rise of temperature for all the studied phosphates. The higher values of thermal diffusivity of the Pb-containing phosphates compared with the Cd-ones are probably associated with larger amplitudes of thermal vibrations of large Pb^{2+} ions in the structure.

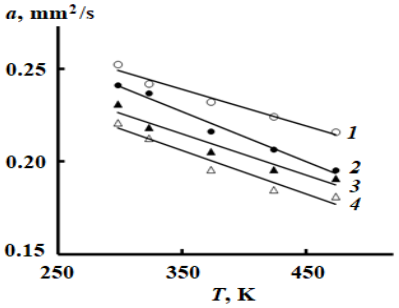

Fig. 9 Thermal diffusivity of the phosphates: $PbMg_{0.5}Zr_{1.5}(PO_4)_3$ (*1*), $Pb_{0.5}Zr_2(PO_4)_3$ (*2*), $Cd_{0.5}Zr_2(PO_4)_3$ (*3*) и $CdMg_{0.5}Zr_{1.5}(PO_4)_3$ (*4*)

For the calculation of thermal conductivity, heat capacity of the Cd-containing phosphates was estimated according to the Dulong and Petit rule, which satisfactorily describes the experimental values for NZP/NASICON phosphates (this work [25]). From the obtained values (Table XIII), the studied phosphates may be characterized as good heat-insulating ceramics (for example, some characteristics of the known refractory material ZrO_2 are: a = 0.57–0.54 mm^2/s, λ = 1.64–1.74 W/(m·K) in the temperature range 298–473 K [26]).

TABLE XIII
THERMAL DIFFUSIVITY AND THERMAL CONDUCTIVITY OF THE PHOSPHATES $M_{0.5+x}Mg_xZr_{2-x}(PO_4)_3$ (M – CD, PB; X = 0, 0.5)

Composition	*a*, mm^2/s 298–473 K	λ, W/(m·K) 473 K
$Cd_{0.5}Zr_2(PO_4)_3$	0.23–0.19	0.33
$CdMg_{0.5}Zr_{1.5}(PO_4)_3$	0.22–0.18	0.33
$Pb_{0.5}Zr_2(PO_4)_3$	0.24–0.20	0.34
$PbMg_{0.5}Zr_{1.5}(PO_4)_3$	0.25–0.22	0.35

IV. CONCLUSIONS

NZP/NASICON type solid solutions were formed in the studied systems of phosphates of zirconium and metals in oxidation degree +2. The obtained results on phase formation, structure and thermophysical properties of the studied compounds may be useful for the development of ceramics with targeted characteristics. Low thermal expansion, heat capacity and thermal conductivity allow us to consider the studied NZP/NASICON materials as promising high-resistant refractories and heat insulators, superior to known materials in their ability to withstand thermal shocks.

REFERENCES

[1] N. Anantharamulu, K. Koteswara Rao, G. Rambabu, B. Vijaya Kumar, Velchuri Radha and M. Vithal, "A wide-ranging review on Nasicon type materials", *J. Mater. Sci.*, vol. 46, no. 9, pp. 2821–2837, May 2011.

[2] M. Guin, F. Tietz and O. Guillon, "New promising NASICON material as solid electrolyte for sodium-ion batteries: Correlation between composition, crystal structure and ionic conductivity of $Na_{3+x}Sc_2Si_xP_{3-x}O_{12}$", *Solid State Ionics*, vol. 293, pp. 18–26, Oct. 2016.

[3] R. P. Forbes, D. H. Barrett, C. B. Rodella and D. G. Billing, "The thermoresponsive behaviour of Nasicon-like $CuTi_2(PO_4)_3$", *Mater.*

Characterization, vol. 155, 109795, Sep. 2019.

[4] S. Chen, C. Wu, L. Shen, C. Zhu, Y. Huang, K. Xi, J. Maier and Y. Yu, "Challenges and perspectives for NASICON-type electrode materials for advanced sodium-ion batteries", *Adv. Mater.*, vol. 29, 1700431, 2017.

[5] L. Vijayan and G. Govindaraj, "NASICON materials: structure and electrical properties", *Polycrystalline Mater. – Theor. and Practical Aspects*, pp. 77–106, Jan. 2012.

[6] P. Knauth, "Inorganic solid Li ion conductors: an overview*", Solid State Ionics*, vol. 180, no. 14-16, pp. 911–916., 2009.

[7] D. K. Agrawal, C.-Y. Huang and H. A. McKinstry, "NZP: a new family of low-thermal expansion materials", *Int. J. Thermophys*., vol. 12, no. 4, pp. 697–710, Jul. 1991.

[8] V. I. Pet'kov and A. I. Orlova, "Crystal-chemical approach to predicting the thermal expansion of compounds in the NZP family", *Inorg. Mater*., vol. 39, no. 10, pp. 1013–1023, Oct. 2003.

[9] A. B. Ilin, N. V. Orekhova, M. M. Ermilova and A. B. Yaroslavtsev, "Catalytic activity of $LiZr_2(PO_4)_3$ NASICON-type phosphates in ethanol conversion process in conventional and membrane reactors*", Catal. Today*, vol. 268, pp. 29–36, Jun. 2016.

[10] Ch. S. Yoon, J. H. Kim, Ch. K. Kim and K. S. Hong, "Synthesis of low thermal expansion ceramics based on $CaZr_4(PO_4)_6$–Li_2O system", *Mater. Science and Eng*., vol. B79, pp. 6–10, Jan. 2001.

[11] E. Breval, H. Mikinstry and D. K. Agrawal, "Synthesis and thermal expansion properties of the $Ca_{(1+x)/2}Sr_{(1+x)/2}Zr_4P_{6-2x}Si_{2x}O_{24}$ system", *J. Am. Ceram. Soc*., vol. 81, no. 4, pp. 926–932, Apr. 1998.

[12] S. Y. Limaye, D. K. Agrawal and H. A. Mckinstry, "Synthesis and thermal expansion of $MZr_4P_6O_{24}$ (M – Mg, Ca, Sr, Ba)", *J. Am. Ceram. Soc.*, vol. 70, no. 10, pp. C232–C236, 1987.

[13] S. Y. Limaye, D. K. Agrawal and R. Roy, "Synthesis, sintering and thermal expansion of $Ca_{1-x}Sr_xZr_4P_6O_{24}$ – an ultra-low thermal expansion ceramic system", *J. Mater. Sci.*, vol. 26, no. 1, pp. 93–98, Jan. 1991.

[14] V. I. Pet'kov, V. S. Kurazhkovskaya, A. I. Orlova and M. L. Spiridonova, "Synthesis and crystal chemical characteristics of the structure of $M_{0.5}Zr_2(PO_4)_3$ phosphates", *Crystallogr. Rep*., vol. 47, no. 5, pp. 736–743, May 2002.

[15] E. Asabina, V. Pet'kov, P. Maiorov, D. Lavrenov, I. Shchelokov and A. Kovalsky, "Synthesis, structure and thermal expansion of the phosphates $M_{0.5+x}M'_xZr_{2-x}(PO_4)_3$ (M, M'− metals in oxidation state +2)", *Pure Appl. Chem*., vol. 89, no. 4, pp. 523-534, Apr. 2017.

[16] P. J. Elving and E. C. Olson, *Analytical Chemistry*, vol. 27, no. 11, pp. 1817-1820, 1955.

[17] R. Brochu, M. El-Yacoubi and M. Louer, "Crystal chemistry and thermal expansion of $Cd_{0.5}Zr_2(PO_4)_3$ and $Cd_{0.25}Sr_{0.25}Zr_2(PO_4)_3$ ceramics", *Mater. Res. Bull*., vol. 32, no. 1, pp. 15-23, Jan. 1997.

[18] P. A. Maiorov, E. A. Asabina, V. I. Pet'kov, E. Yu. Borovikova and A. M. Koval'skii, "Complex phosphates $M_{0.5+x}M'_xZr_{2-x}(PO_4)_3$ (M = Cd, Sr, Pb; M′ = Ni, Cu; $0 \le x \le 2$) with an-NZP Type Structure", *Rus. J. Inorg. Chem*., vol. 64, no. 6, pp. 710–716, Jun. 2019.

[19] Y. I. Kim and F. Izumi, "Structure Refinements with a New Version of the Rietveld-Refinement Program RIETAN", *J. Ceram. Soc. Jpn.*, vol. 102, no. 1184, pp. 401–404, Apr. 1994.

[20] R. M. Varushchenko, A. I. Druzhinina and E. L. Sorkin, "Low-temperature heat capacity of 1-bromoperfluorooctane", *J. Chem. Thermodyn*., vol. 29, no. 6, pp. 623-637, Jun. 1997.

[21] G. W. H. Hohne, W. F. Hemminger and H.-J. Flammersheim, "Differential Scanning Calorimetry, second ed.", *Springer-Verlag Berlin Heidelberg GmbH*, New York, 2003.

[22] V. A. Drebushchak, "Calibration coefficient of a heat-flow DSC; Part II. Optimal calibration procedure", *J. Therm. Anal. Calorim*., vol. 79, no. 1, pp. 213-218, Jan. 2005.

[23] A. Mouline, M. Alami, R. Brochu and R. Olazcuaga," Structural and luminescent properties of a Nasicon-type phosphate $Cu^{I}_{0.5}Mn^{II}_{0.25}Zr_2(PO_4)_3$", *J. Solid State Chem*., vol. 152, no. 2, pp. 453–459, Jul. 2000.

[24] S. A. Larregola, J. A. Alonso, M. Alguero, R. Jiménez, E. Suard, F. Porcher and J. C. Pedregosa, "Effect of the Pb^{2+} lone electron pair in the structure and properties of the double perovskites $Pb_2Sc(Ti_{0.5}Te_{0.5})O_6$ and $Pb_2Sc(Sc_{0.33}Te_{0.66})O_6$: relaxor state due to intrinsic partial disorder", *Dalton Trans*., vol. 39., no. 21, pp. 5159–5165, Jun. 2010.

[25] V. I. Pet'kov and E. A. Asabina, "Thermodynamic properties of compounds with kosnarite-type structure", *Ind. J. Chem*., vol. 52A, no. 3, pp. 350–356, March 2013.

[26] V. Ya. Shevchenko and S. M. Barinov, "Engineering Ceramics", Moscow, Nauka, 1993.